

Supplementary Information

Title: **Broadband visible-near infrared and deep ultraviolet generation by four-wave mixing and high-order stimulated Raman scattering from hybrid metasurfaces of plasmonic nanoantennae and Raman active nanoparticles**

Wi-Song Rim^{a,b} and Kwang-Hyon Kim^{a,}*

^aInstitute of Physics, State Academy of Sciences, Unjong District, Pyongyang, Democratic People's Republic of Korea

^bInstitute of Lasers, State Academy of Sciences, Unjong District, Pyongyang, Democratic People's Republic of Korea

* E-mail: kwang-h.kim@star-co.net.kp

S1. Modeling the Raman and Kerr nonlinearity of diamond

We have used Raman-Kerr model for the nonlinear responses provided by Lumerical FDTD Solutions [S1]. Taking into account the contributions of both Raman and Kerr nonlinearities, the total polarization can be described by

$$P(t) = \varepsilon_0 \chi^{(1)} E(t) + \varepsilon_0 \chi_{\text{Kerr}}^{(3)} E^3(t) + \varepsilon_0 E(t) \left[\chi_R^{(3)}(t) * E^2(t) \right], \quad (\text{S1})$$

where ε_0 is the vacuum permittivity, $E(t)$ is the electric field of light, $\chi^{(1)}$ is the linear susceptibility, $\chi_{\text{Kerr}}^{(3)} = \alpha \chi_0^{(3)}$ is the third-order susceptibility representing the Kerr nonlinearity, α is a constant in the interval $0 < \alpha < 1$, $\chi_0^{(3)}$ is the total third-order nonlinear susceptibility, $\chi_R^{(3)}(t)$ is the contribution of Raman process to the third-order susceptibility given in time domain, and $*$ denotes the convolution operator, respectively. The third-order susceptibility $\chi_R^{(3)}(\Omega)$ responsible for Raman process in frequency domain is

$$\chi_R^{(3)}(\Omega) = \frac{(1-\alpha)\chi_0^{(3)}\Omega_R^2}{\Omega_R^2 + 2i\Omega\delta_R - \Omega^2}, \quad (\text{S2})$$

where $\Omega_R = 2\pi\tilde{\nu}c$, $\tilde{\nu}$ is the Raman shift in the unit of m^{-1} , c is the light velocity in vacuum, $\delta_R = 2\pi\Delta\tilde{\nu}c$, $\Delta\tilde{\nu}$ is the linewidth of Raman gain in the unit of m^{-1} , $\Omega = \omega_L - \omega_S$, ω_L and ω_S are the angular frequencies of pump and Stokes Raman waves. $\chi_R^{(3)}(t)$ is the inverse Fourier transform of $\chi_R^{(3)}(\omega)$.

The imaginary part of the Raman susceptibility is related to the Raman gain g_R through [S2]

$$\text{Im} \left[\chi_R^{(3)} \right]_{\Omega=\Omega_R} = -\frac{n_L n_S g_R}{2\mu_0 \omega_S}, \quad (\text{S3})$$

where n_L and n_S are the refractive indices at pump and Stokes Raman wavelengths, μ_0 is the permeability of vacuum, respectively. From Eqs. (S2) and (S3), we get $(1-\alpha)\chi_0^{(3)} =$

$n_L n_S \delta_R g_R / \mu_0 \omega_S \Omega_R$. From the above equations, we have the following parameters necessary for numerical modeling of Raman process:

$$\begin{cases} \chi_0^{(3)} = \chi_{\text{Kerr}}^{(3)} + \frac{n_L n_S \delta_R g_R}{\mu_0 \omega_S \Omega_R}, \\ \alpha = \chi_{\text{Kerr}}^{(3)} / \chi_0^{(3)}. \end{cases} \quad (\text{S4})$$

By using the above equation and $\chi_{\text{Kerr}}^{(3)} = 2.5 \times 10^{-21} \text{ m}^2 \text{V}^{-2}$ (see main text), we obtain $\alpha = 0.8851$ and $\chi_0^{(3)} = 2.8244 \times 10^{-21} \text{ m}^2 \text{V}^{-2}$ at $\lambda_L = 800 \text{ nm}$, being $\omega_L = 2\pi c / \lambda_L$. Here the other parameters for diamond are $g_R = 2.65 \times 10^{-10} \text{ m/W}$ (see main text), $\tilde{\nu} = 1332.5 \text{ cm}^{-1}$ [S3], $\Delta\tilde{\nu} = 1.5 \text{ cm}^{-1}$ [S2], $n_L = 2.3975$, and $n_S = 2.3965$ [S4], respectively. We have compiled plugin codes of chi3ramankerr [S1] and added as a user-defined material model to Lumerical FDTD for numerical modeling of Raman and Kerr responses of diamond.

S2. Nonlinear efficiencies of major spectral peaks generated by four-wave mixing (FWM) and high-order stimulated Raman scattering (HSRS)

From the result shown in Fig. 3, we can calculate the efficiencies of spectral peaks, which are presented in the following table. In the table, ω_0 and $\omega_0 - \Omega_R$ are the central angular frequencies of two incident pulses, and Ω_R represents the Raman shift.

Table 1. Nonlinear generation efficiencies of major spectral peaks. In the left column, both contributions of HSRS and FWM are considered (HSRS + FWM), while in the right column only the contribution of FWM (FWM only) is taken into account.

Frequency	λ (nm)	Efficiency (%)	
		HSRS+FWM	FWM only
$\omega_0 - 3\Omega_R = 2(\omega_0 - \Omega_R) - (\omega_0 + \Omega_R)$	1176.1	1.0813×10^{-5}	3.5778×10^{-6}
$\omega_0 - 2\Omega_R = 2(\omega_0 - \Omega_R) - \omega_0$	1016.8	6.3624×10^{-2}	1.3020×10^{-2}
$\omega_0 + \Omega_R = 2\omega_0 - (\omega_0 - \Omega_R)$	722.9	6.5345×10^{-2}	1.7887×10^{-2}
$\omega_0 + 2\Omega_R = 2\omega_0 - [(\omega_0 - \Omega_R) - \Omega_R]$	659.4	3.1504×10^{-4}	3.7599×10^{-5}
$\omega_0 + 3\Omega_R = 2(\omega_0 + \Omega_R) - (\omega_0 - \Omega_R)$	606.2	1.1249×10^{-6}	9.3816×10^{-7}
$3\omega_0 - 5\Omega_R = 2(\omega_0 - \Omega_R) + [(\omega_0 - \Omega_R) - 2\Omega_R]$	324.4	7.9107×10^{-8}	5.6246×10^{-8}
$3\omega_0 - 4\Omega_R = 2(\omega_0 - \Omega_R) + [(\omega_0 - \Omega_R) - \Omega_R]$	310.8	1.1621×10^{-7}	7.3750×10^{-8}
$3\omega_0 - 3\Omega_R = 3(\omega_0 - \Omega_R)$	298.5	2.1038×10^{-4}	1.3972×10^{-4}
$3\omega_0 - 2\Omega_R = \omega_0 + 2(\omega_0 - \Omega_R)$	287.1	1.0520×10^{-3}	1.0181×10^{-3}
$3\omega_0 - \Omega_R = 2\omega_0 + (\omega_0 - \Omega_R)$	276.5	4.6146×10^{-4}	6.3731×10^{-4}
$3\omega_0$	266.7	1.1622×10^{-5}	2.4802×10^{-5}
$3\omega_0 + \Omega_R = 2\omega_0 + (\omega_0 + \Omega_R)$	257.5	8.7501×10^{-7}	6.6303×10^{-7}
$3\omega_0 + 2\Omega_R = 2\omega_0 + (\omega_0 + 2\Omega_R)$	249.0	4.2088×10^{-8}	1.6563×10^{-8}

S3. Reflection spectra for different pump intensities

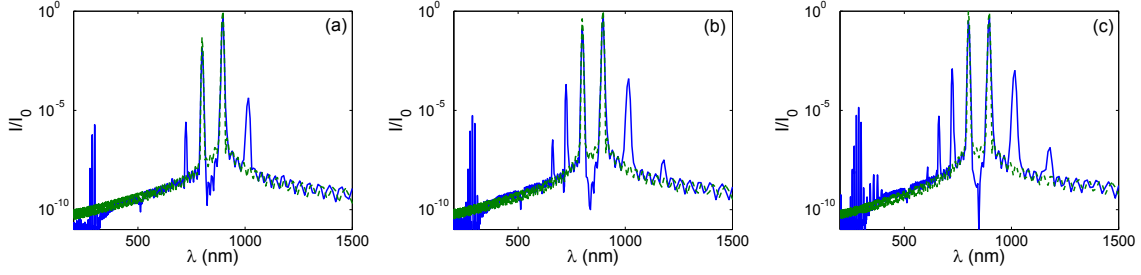


Figure S1. Reflection spectra from the metasurface of silver nanoantenna array embedded with diamond nanoparticles. The structural and material parameters are the same as in Fig. 3. Peak intensity of the pump at 895.46 nm is $I_2 = 33.18 \text{ GW/cm}^2$. Peak intensities of the pump at 800 nm are $I_1 = 1.33 \text{ GW/cm}^2$, (a), 11.94 GW/cm^2 (b), and 33.18 GW/cm^2 (c), respectively.

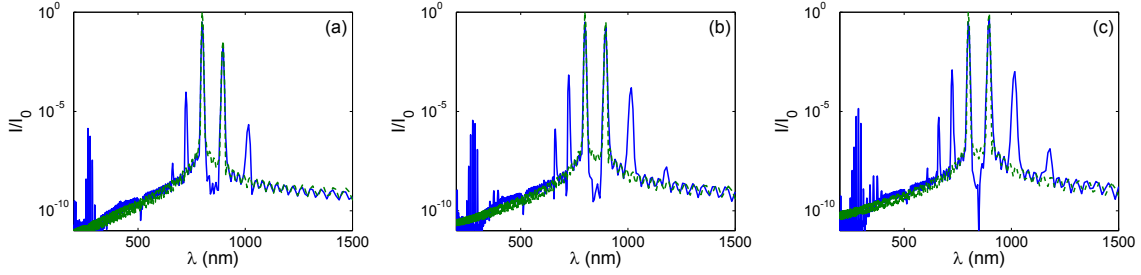


Figure S2. Reflection spectra from the metasurface of silver nanoantenna array embedded with diamond nanoparticles. The structural and material parameters are the same as in Fig. 3. Peak intensity of the pump at 800 nm is $I_1 = 33.18 \text{ GW/cm}^2$. Peak intensities of the pump at 895.46 nm are $I_2 = 1.33 \text{ GW/cm}^2$ (a), 11.94 GW/cm^2 (b), and 33.18 GW/cm^2 (c), respectively.

S4. Reflection spectra for different pump wavelengths

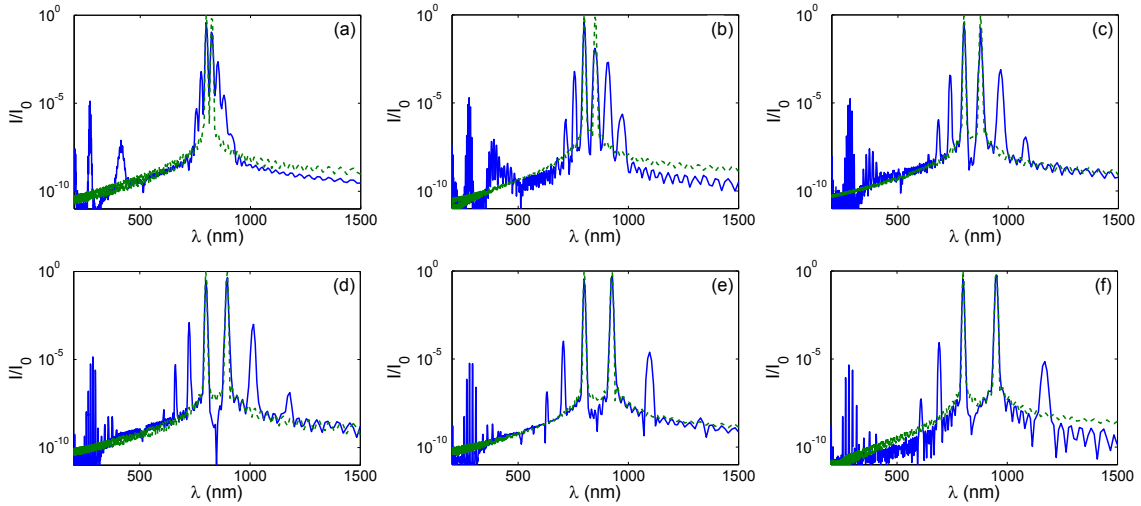


Figure S3. Reflection spectra for different wavelength λ_2 of the pump at $\omega_0 - \Delta\omega$. The values of λ_2 are 825 nm (a), 850 nm (b), 875 nm (c), 895.46 nm (d), 925 nm (e), and 950 nm (f), respectively. The central wavelength of the other pump at ω_0 is fixed to 800 nm. Other conditions are the same as in Fig. 3. When $\lambda_2 = 895.46$ nm in (d), the frequency difference between the pumps is identical to Raman shift.

References

[S1] <https://kb.lumerical.com>.

[S2] R. P. Mildren, Intrinsic Optical Properties of Diamond, in *Optical Engineering of Diamond*, ed. by R. P. Mildren and J. R. Rabeau, Wiley-VCH, Weinheim, 2013.

[S3] A. A. Kaminskii, R. J. Hemley, J. Lai, C. S. Yan, H. K. Mao, V. G. Ralchenko, H. J. Eichler and H. Rhee, High-Order Stimulated Raman Scattering in CVD Single Crystal Diamond, *Laser Phys. Lett.*, 2007, **4**, 350-353.

[S4] E. D. Palik, *Handbook of Optical Constants of Solid*, Academic Press, New York, 1985.